MRC

Received: 29 October 2015 Revised: 3 January 2016 Accepted: 7 January 2016 Published online in Wiley Online Library: 11 February 2016

(wileyonlinelibrary.com) DOI 10.1002/mrc.4414

The synthesis, structural elucidation and antimicrobial activity of 2- and 4-substituted-coumarinyl chalcones

Thrineshen Moodley,[a] Mehbub Momin,[a] Chunderika Mocktar,[b] Christina Kannigadu[a] and Neil A. Koorbanally[a]*

Introduction

Coumarinyl chalcones are hybrid molecules combining the skeletal frameworks of coumarins (aromatic lactones) and chalcones (aromatic α,β-unsaturated carbonyl compounds). Both these skeletal frameworks are found abundantly in nature and may have a role to play in the medicinal effects of the extracts of plants.[1–4] Because both coumarins and chalcones each have a variety of medicinal properties,[5–9] combining both these pharmacophores into one molecule could result in either enhanced activity of each of their properties individually or a broader spectrum of medicinal properties than either of them on their own.

These hybrid heterocyclic molecules were first synthesized from 3-acetyl coumarin and substituted benzaldehydes[10] by the Claisen–Schimdt condensation carried out in an alcoholic solvent and using either an ionic or organic base.[11,12] This has been a popular method for synthesizing coumarinyl chalcones;[13–15] however, variations such as microwave solvent free synthesis have been carried out with decreased reactions times and optimized yields.[16] Although the preferred method has been to use bases such as sodium hydroxide and piperidine, a greener approach involving cellulose sulphonic acid as a catalyst was also employed.[17]

Hybrid coumarinyl chalcones have recently shown anticancer,[18] antioxidant,[19] analgesic,[20] antiinflammatory[20] and antibacterial activity[19–21] and when complexed with Ni and Cu together with fluoroquinolones, played a part in developing highly active anticancer and antioxidant complexes.[22] This is not surprising, because the two pharmacophores individually have shown activity in all these assays.[23–28]

To our knowledge, there have been no reports on docking studies with coumarinyl chalcones to any of the known protein targets which we have used in this work; however, chalcones themselves have been docked to the HIV-integrase enzyme[29] and the colchine region of tubulin,[30] where the carbonyl group was found to be essential for docking. Coumarins have been docked to the COX-1 and COX-2 enzymes[31] and the metabolic enoyl-ACP-reductase enzyme of bacteria.[32] There are no reports of coumarinyl chalcones being docked to the penicillin binding protein 2X (PBP 2X) used in this study.

We herein report the synthesis and antibacterial activity of coumarinyl chalcones and explore the effect that chloro, fluoro, hydroxy, methoxy and prenyl groups have on activity as well as determine which of the 2 or 4 positions were better for substitution with regard to antibacterial activity and investigate the possible synergistic binding affinity that the coumarin and chalcone moieties possess when incorporated onto the same backbone using molecular docking.

Experimental

General experimental procedures

^{1}H and ^{13}C NMR spectra were recorded at 298 K with 5–10 mg samples dissolved in 0.5 ml $CDCl_3$ in 5 mm NMR tubes using a Bruker Avance^{III} 400 MHz NMR spectrometer (9.4 T; Bruker, Germany) (400.22 MHz for ^{1}H and 100.63 MHz for ^{13}C. The digital digitizer resolution was set at 22 for both the ^{1}H and ^{13}C NMR experiments. Chemical shifts (δ) are reported in parts per million and coupling constants (J) in hertz. The ^{1}H and ^{13}C chemical shifts of the deuterated solvent were 7.24 and 77.0 respectively, referenced to the internal standard, TMS. For the ^{1}H NMR analyses, 16 transients were acquired with a 1 s relaxation delay using 32 K data points. The 90° pulse duration was 10.0 μs, and the spectral width was 8223.68 Hz. The ^{13}C NMR spectra were obtained with a spectral width of 24 038.46 Hz using 64 K data points. The 90° pulse duration was 8.40 μs. For the two-dimensional experiments including COSY, NOESY, HSQC and HMBC, all data were acquired with 4 K × 128 data points ($t_2 \times t_1$). The mixing time for the NOESY experiment was 0.3 s, and the long-range coupling time for the HMBC experiment was 65 ms. All data were analysed using Bruker Topspin 2.1 (2008) software.

Reagent grade chemicals used in this study were purchased from Sigma Aldrich, South Africa. IR spectra were recorded on a Perkin Elmer Spectrum 100 FTIR spectrometer with universal ATR sampling accessory. For GC-MS, the samples were analysed on an Agilent GC-MSD apparatus equipped with DB-5SIL MS (30 × 0.25 mm i.d., 0.25 μm film thickness) fused-silica capillary

* *Correspondence to: Neil A. Koorbanally, School of Chemistry and Physics, University of KwaZulu-Natal, Private Bag X54001, Durban 4000, South Africa. E-mail: Koorbanally@ukzn.ac.za*

a *School of Chemistry and Physics, University of KwaZulu-Natal, Durban, South Africa*

b *Discipline of Pharmaceutical Science, School of Health Science, University of Kwazulu-Natal, Durban, South Africa*

column. Helium (at 2 ml min^{-1}) was used as a carrier gas. The MS was operated in the EI mode at 70 eV. Melting points were recorded on an Ernst Leitz Wetzlar micro-hot-stage melting point apparatus. HRMS was carried out on a Bruker microTOF-Q II ESI instrument operating at ambient temperatures, with a sample concentration of 1 ppm. Column chromatography was carried out on a 2 cm column with silica gel as the stationary phase and varying solvent ratios of ethyl acetate and hexane as the mobile phase. Samples of 60 ml were collected for each fraction and masses typically between 0.5 and 1.0 g were loaded onto the column.

Synthesis

Chalcone (1,3-diphenylprop-2-enone) was also prepared according to a published method in the literature because we wanted to compare the activity results with this basic skeleton. The structure was verified by NMR spectroscopy according to an authentic sample available in the laboratory.[33]

Preparation of 3-acetyl-2H-chromen-2-one (1)

2-Hydroxybenzaldehyde (83.14 mmol, 10.07 g) and ethylacetoacetate (77.07 mmol, 10.03 g) was added to a solution of absolute ethanol (50.0 ml). A catalytic amount of piperidine (10 drops) was then added dropwise with cooling. The reaction was left to stir for 16 h at room temperature. The resulting precipitate was filtered and recrystallized with glacial acetic acid to produce a light yellow solid precipatate in 90% yield. ^{1}H NMR (400 MHz, $CDCl_3$): δ 2.71 (CH_3), 7.33 (m, H-6′/8′), 7.62 (m, H-5′/7′), 8.47 (s, H-4′). ^{13}C NMR (100 MHz, $CDCl_3$): δ 30.5 (CH_3), 116.6 (C-8′), 118.3 (C-4a′), 124.5 (C-3′), 125.0 (C-6′), 130.2 (C-5′), 134.4 (C-7′), 147.5 (C-4′), 155.3 (C-8a′), 159.3 (C-2′), 195.5 (C-9′).

Preparation of (3-methylbut-2-enyloxy)benzaldehyde intermediates (2k and 2l)

2-Hydroxybenzaldehyde or 4-hydroxybenzaldehyde (8.19 mmol, 1.00 g) was added to a solution of dry acetone (100 ml) followed by the addition of anhydrous potassium carbonate (3.05 g). 1-Bromo-3-methyl-2-butene (prenyl bromide) (16.77 mmol, 2.5 g) was then added dropwise, and the reaction stirred at room temperature for 3 h. On completion, the acetone was removed under reduced pressure and the resulting crude solid washed with water and extracted with 3 × 20 ml portions of diethyl ether. The diethyl ether extract was concentrated and purified using column chromatography with 8:2 hexane : ethyl acetate to yield 0.75 g of **2k** and 1.05 g of **2l** respectively.

2-(3-methylbut-2-enyloxy)benzaldehyde (**2k**) brown oil (50% yield); ^{1}H NMR (400 MHz, $CDCl_3$) δ 1.73 (CH_3), 1.78 (CH_3), 4.61 (d, J = 6.0 Hz, CH_2), 5.47 (t, J = 6.0 Hz, =CH), 6.97 (2H, m, H-3/5), 7.50 (t, 7.0 Hz, H-4), 7.80 (d, J = 7.0 Hz, H-6), 10.4 (s, CHO); ^{13}C NMR (100 MHz, $CDCl_3$): δ 18.4 (CH_3), 26.0 (CH_3), 65.5 (CH_2), 113.1 (C-3), 119.1 (=CH), 120.5 (C-5), 125.1 (C-1), 128.3 (C-4), 135.9 (C-6), 138.6 (=C), 161.5 (C-2), 190.0 (CHO).

4-(3-methylbut-2-enyloxy)benzaldehyde (**2l**) brown oil (60% yield); ^{1}H NMR (400 MHz, $CDCl_3$): δ 1.73 (CH_3), 1.78 (CH_3), 4.57 (d, J = 6.0 Hz, CH_2), 5.47 (t, J = 6.0 Hz, =CH), 6.98 (d, J = 8.0 Hz, 2H, H-3/5), 7.79 (d, J = 8.0 Hz, 2H, H-2/6), 9.85 (s, CHO); ^{13}C NMR (100 MHz, $CDCl_3$): δ 18.05 (CH_3), 25.64 (CH_3), 65.1 (CH_2), 115.0 (2C, C-3/5), 118.79 (=CH), 129.7 (C-1), 131.9 (2C, C-2/6), 139.0 (=C), 163.85 (C-4), 190.8 (CHO).

Preparation of 3-acetyl-2H-chromen-2-ones (3a–l)

The synthesized 3-acetyl coumarin (5.31 mmol, 1.00 g) was added to absolute ethanol (50 ml) with stirring, followed by the addition of benzaldehydes **2a–l** (10.62 mmol). A catalytic amount of piperidine (10 drops) was then added and the reaction left to reflux for 5 h. On cooling, a yellow precipitate formed, which was then filtered under vacuum and recrystallized in absolute ethanol to yield compounds **3a–l** with purities of between 78 and 99%.

(E)-3-(3-phenyl)-prop-2-enoyl)-2H-chromen-2-one (***3a***) light yellow solid; 90% yield; mp 130–132 °C; UV λ_{max} nm (log ε): 297 (2.86), 333 (2.69); IR υ_{max} (cm^{-1}): 1725 (O–C=O), 1656 (C=O), 1555 (C=C); EIMS *m/z* (rel. int.) 276 (100) [M^+], 248 (39), 231 (20), 131 (60), 103 (96), 77 (62).

(E)-3-(3-(2-methoxyphenyl)-prop-2-enoyl)-2H-chromen-2-one (***3b***) bright yellow solid; 80% yield; mp 126–128 °C; UV λ_{max} nm (log ε): 303 (3.30), 347 (3.32); IR υ_{max} (cm^{-1}): 1714 (O–C=O), 1654 (C=O), 1552 (C=C); EIMS *m/z* (rel. int.) 306 (12) [M^+], 275 (100), 247 (4), 231 (11), 161 (11), 131 (3).

(E)-3-(3-(4-methoxyphenyl)-prop-2-enoyl)-2H-chromen-2-one (***3c***) bright yellow solid; 85% yield; mp 130–132 °C; UV λ_{max} nm (log ε): 280 (4.64), 372 (4.98); IR υ_{max} (cm^{-1}): 1717 (O–C=O), 1658 (C=O), 1555 (C=C); EIMS *m/z* (rel. int.) 306 (100) [M^+], 278 (15), 263 (20), 161 (45), 133 (45), 108 (32).

(E)-3-(3-(2,4-dimethoxyphenyl)-prop-2-enoyl)-2H-chromen-2-one (***3d***) bright yellow solid; 93% yield; mp 150–153 °C; UV λ_{max} nm (log ε): 303 (3.06), 372 (3.21); IR υ_{max} (cm^{-1}): 1711 (O–C=O), 1654 (C=O), 1552 (C=C); EIMS *m/z* (rel. int.) 337 (11) [M^+], 336 (56), 305 (100), 277 (2), 191 (23), 148 (27).

(E)-3-(3-(2-chlorophenyl)-prop-2-enoyl)-2H-chromen-2-one (***3e***) light yellow solid; 78% yield; mp 140–142 °C; UV λ_{max} nm (log ε): 305 (4.14), 332 (4.15); IR υ_{max} (cm^{-1}): 1718 (O–C=O), 1685 (C=O), 1555 (C=C); EIMS *m/z* (rel. int.) 275 [$M^+ - Cl$] (100), 247 (8), 231 (12), 165 (7), 137 (19), 101 (32).

(E)-3-(3-(4-chlorophenyl)-prop-2-enoyl)-2H-chromen-2-one (***3f***) light yellow solid; 82% yield; mp 153–155 °C; UV λ_{max} nm (log ε): 300 (4.34), 333 (4.39); IR υ_{max} (cm^{-1}): 1714 (O–C=O), 1666 (C=O), 1557 (C=C); EIMS *m/z* (rel. int.) 310 (100) [M^+], 282 (76), 275 (23), 266 (14), 247 (38), 165 (57), 137 (76), 101 (92).

(E)-3-(3-(2-fluorophenyl)-prop-2-enoyl)-2H-chromen-2-one (***3g***) yellow solid; 80% yield; mp 153–155 °C; UV λ_{max} nm (log ε): 328 (4.34), 370 (4.43); IR υ_{max} (cm^{-1}): 1722 (O–C=O), 1682 (C=O), 1557 (C=C); EIMS *m/z* (rel. int.) 294 (80) [M^+], 266 (73), 249 (8), 149 (69), 121 (76), 101 (100); HRMS: [M^+ + Na] at *m/z* 317.0596 (Calculated for $C_{18}H_{11}O_3FNa$, 317.0590).

(E)-3-(3-(4-fluorophenyl)-prop-2-enoyl)-2H-chromen-2-one (***3h***) yellow solid; 80% yield; mp 142–145 °C; UV λ_{max} nm (log ε): 300 (4.38), 350 (4.38); IR υ_{max} (cm^{-1}): 1715 (O–C=O), 1676 (C=O), 1556 (C=C); EIMS *m/z* (rel. int.) 294 (80) [M^+], 266 (73), 265 (40), 249 (19), 149 (69), 121 (76), 101 (100).

(E)-3-(3-(2-hydroxyphenyl)-prop-2-enoyl)-2H-chromen-2-one (***3i***) yellow solid; 75% yield; mp 158–161 °C; UV λ_{max} nm (log ε): 247 (4.01), 342 (4.39); IR υ_{max} (cm^{-1}): 3341 (OH), 1700 (O–C=O), 1651 (C=O), 1571 (C=C); EIMS *m/z* (rel. int.) 292 (100) [M^+], 264 (30), 247 (20), 147 (61), 119 (46), 91 (68).

(E)-3-(3-(4-hydroxyphenyl)-prop-2-enoyl)-2H-chromen-2-one (***3j***) yellow solid; 88% yield; mp 188–190 °C; UV λ_{max} nm (log ε): 310 (4.28), 360 (4.45); IR υ_{max} (cm^{-1}): 3294 (OH), 1698 (O–C=O), 1650

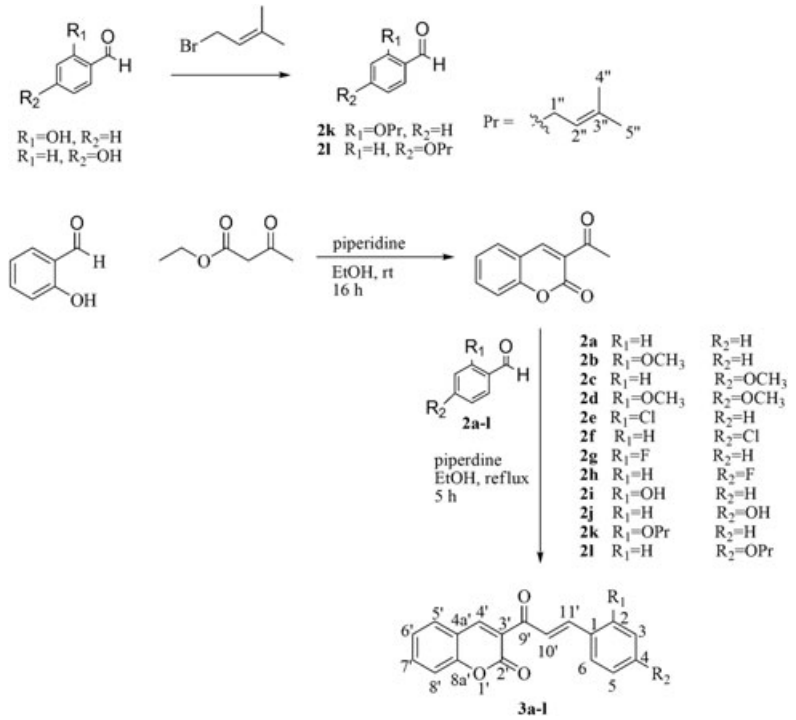

Scheme 1. Synthesis of 2- and 4- substituted coumarinyl chalcones.

(C=O), 1550 (C=C); EIMS *m/z* (rel. int.) 292 (100) [M^+], 264 (25), 247 (18), 147 (46), 119 (43), 91 (54).

(E)-3-(3-(2-(3-methylbut-2-enyloxy)phenyl)-prop-2-enoyl)-2H-chromen-2-one (***3k***) yellow solid; 80% yield; mp 92–95 °C; UV λ_{max} nm (log ε): 312 (4.35), 363 (4.46); IR υ_{max} (cm^{-1}): 1727 (O–C=O), 1606 (C=O), 1559 (C=C); EIMS *m/z* (rel. int.) 360 (19) [M^+], 327 (15), 173 (100), 146 (19); HRMS: [M^+ + Na] at *m/z* 383.1268 (Calculated for C_{23} $H_{20}O_4Na$, 383.1259).

(E)-3-(3-(4-(3-methylbut-2-enyloxy)phenyl)-prop-2-enoyl)-2H-chromen-2-one (***3l***) yellow solid; 89% yield; mp 119–121 °C; UV λ_{max} nm (log ε): 295 (4.01), 376 (4.21); IR υ_{max} (cm^{-1}): 1719 (O–C=O), 1660 (C=O), 1567 (C=C); EIMS *m/z* (rel. int.) 360 (10) [M^+], 292 (100), 173 (34), 147 (40), 67 (50); HRMS: [M^+ + Na] at *m/z* 383.1269 (Calculated for $C_{23}H_{20}O_4Na$, 383.1259).

Antibacterial assay

Microbial strains

The antimicrobial activity of the synthesized compounds **3a–3l,** its precursor, 3-acetylcoumarin and chalcone (1,3-diphenylprop-2-enone) were tested against two Gram-positive bacteria, *Staphylococcus aureus* 29263 and *S. aureus* Rosenbach ATCC BAA-1683 (methicillin resistant *S. aureus*) and two Gram-negative bacteria, *Klebsiella pneumonia* ATCC 31488 and *Escherichia coli* ATCC 25922 as well as one fungal species, *Candida albicans* ATCC 10231, according to the disc diffusion method.

Disc diffusion method

The standard antibiotics ciprofloxacin and ampicillin were used as controls for comparison. Mueller Hilton agar was prepared (38 g in 1 l of water), poured into sterile prelabeled petri dishes and allowed to set and dry at room temperature. Bacterial or fungal organisms were standardized using a 0.5 McFarland standard turbidity and then swabbed onto agar plates. Paper discs were dissolved in sample at concentrations of between 99 and 101 μg for the coumarinyl chalcones and chalcone itself and at 99 μg for 3-acetylcoumarin and placed onto the prepared agar plates which were inverted and incubated at 35–37 °C for 24 h. The diameter of the zone of inhibition was measured in millimetres. Compounds **3c–e**, **3g** and **3i** as well as chalcone showed inhibition zones of >3 mm and were selected to determine their minimum bactericidal concentration (MBC) values using the broth microdilution assay with ampicillin as the control and following the method in Andrews.[34]

Broth dilution method

Compounds **3c–3e**, **3g** and **3i** and chalcone was dissolved in DMSO (10 mg ml^{-1}) and serially diluted 5 times with Mueller–Hinton broth, inoculated with the respective bacterial cultures and incubated at 37 °C for 18 h. This was performed in duplicate. Thereafter, 10 μl from each concentration was placed on Mueller–Hinton plates and incubated at 37 °C for 18 h to determine the MBC. The MBC was the lowest concentration, which showed no bacterial growth in the area in which the sample was placed.

Molecular docking studies

The crystal structure of Cefditoren (CDS) bound to the active site of PBP 2X was obtained from the Protein Data Bank (http://www.rscb.org/pdb) with the PDB ID: **2Z2M**. Co-crystallized ligands were identified and removed from the target proteins, and crystallographic water molecules were eliminated from the 3D coordinate file. A geometry optimization of all the compounds was performed by Gaussian 2009 software[35] by the semiempirical method PM6 for flexible conformation of the compounds during docking. A grid box (including residues within a 10.0 Å radius) large enough to accommodate the active site was constructed

Table 1. ^{1}H NMR data (δ in ppm) of coumarinyl chalcones **3a–l** (400 MHz, $CDCl_3$, *J* is given in Hz)

No.	3a	3b	3c	3d	3e	3f	3g	3h	3i[a]	3j[a]	3k	3l
OCH_3	—	3.90 (s)	3.83 (s)	3.91 (s) *ortho* 3.87 (s) *para*	—	—	—	—	—	—	—	
4′	8.56 (s)	8.51 (s)	8.54 (s)	8.54 (s)	8.58 (s)	8.61 (s)	8.56 (s)	8.60 (s)	8.65 (s)	8.61 (s)	8.55 (s)	8.59 (s)
5′	7.61–7.66 (m)	7.58–7.67 (m)	7.60–7.65 (m)	7.62–7.68 (m)	7.62–7.67 (m)	7.66–7.70 (m)	7.62–7.67 (m)	7.65–7.70 (m)	7.94 (d, 8.2)	7.92 (dd, 8.2, 1.5)	7.63–7.71 (m)	7.63–7.69 (m)
6′	7.33 (td, 7.6, 1.0)	7.29–7.36 (m)	7.32 (dd, 6.48)	7.34 (dd, 6.6)	7.26–7.42 (m)	7.35–7.42 (m)	7.32–7.39 (m)	7.37 (dd, 7.4)	7.42 (dd, 8.2)	7.42 (t, 8.2)	7.33–7.40 (m)	7.36 (dd, 7.4)
7′	7.61–7.66 (m)	7.58–7.67 (m)	7.60–7.65 (m)	7.62–7.68 (m)	7.62–7.67 (m)	7.66–7.70 (m)	7.62–7.67 (m)	7.65–7.70 (m)	7.74 (dd, 8.2)	7.74 (td, 8.2, 1.0)	7.63–7.71 (m)	7.63–7.69 (m)
8′	7.38–7.40 (m)	7.29–7.36 (m)	7.37 (d, 9.7)	7.39 (d, 7.5)	7.26–7.42 (m)	7.35–7.42 (m)	7.32–7.39 (m)	7.41 (d, 8.6)	7.48 (d, 8.2)	7.48 (d, 8.2)	7.33–7.40 (m)	7.41 (d, 7.4)
10′	7.93 (d, 15.8)	7.93 (d, 15.1)	7.79 (d, 15.3)	7.89 (d, 15.0)	7.91 (d, 15.5)	7.95 (d, 15.3)	7.96 (d, 15.5)	7.90 (d, 15.4)	7.71 (d, 15.9)	7.44 (d, 15.4)	7.98 (d, 15.6)	7.82 (d, 15.6)
11′	7.85 (d, 15.8)	8.19 (d, 15.1)	7.84 (d, 15.3)	8.17 (d, 15.0)	8.25 (d, 15.5)	7.82 (d, 15.3)	8.02 (d, 15.5)	7.83 (d, 15.4)	7.97 (d, 15.9)	7.69 (d,15.4)	8.24 (d, 15.6)	7.89 (d, 15.6)
2	7.61–7.66 (m)	—	7.61 (d, 8.7)	—	—	7.62 (d, 8.8)	—	7.65–7.70 (m)	—	7.61 (d, 8.7)	—	7.63–7.69 (m)
3	7.38–7.40 (m)	6.89 (d, 8.6)	6.89 (d, 8.7)	6.46 (d, 2.6)	7.26–7.42 (m)	7.39 (d, 8.8)	7.09 (dd, 10.2, 8.4)	7.11 (t, 8.7)	6.93 (d, 7.0)	6.82 (d, 8.7)	6.93 (d, 9.0)	6.95 (d, 9.0)
4	7.38–7.40 (m)	7.29–7.36 (m)	—	—	7.26–7.42 (m)	—	7.32–7.39 (m)	—	7.28 (dd, 7.0)	—	7.33–7.40 (m)	—
5	7.38–7.40 (m)	6.95 (t, 7.8)	6.90 (d, 8.7)	6.55 (dd, 8.4, 2.6)	7.26–7.42 (m)	7.39 (d, 8.8)	7.17 (t, 7.9)	7.11 (t, 8.7)	6.87 (t, 7.0)	6.82 (d, 8.7)	6.98 (t, 8.2)	6.95 (d, 9.0)
6	7.61–7.66 (m)	7.58–7.67 (m)	7.61 (d, 8.7)	7.65 (dd, 8.4, 2.6)	7.81 (dd, 8.0, 1.8)	7.62 (d, 8.8)	7.71 (td, 7.9, 2.0)	7.65–7.70 (m)	7.63 (d, 7.0)	7.61 (d, 8.7)	7.63–7.71 (m)	7.63–7.69 (m)
1″	—	—	—	—	—	—	—	—	—	—	4.63 (d, 7.2)	4.57 (d, 6.5)
2″	—	—	—	—	—	—	—	—	—	—	5.56 (t, 7.2)	5.50 (t, 6.5)
4″	—	—	—	—	—	—	—	—	—	—	1.76 (s)	1.77 (s)
5″	—	—	—	—	—	—	—	—	—	—	1.82 (s)	1.82 (s)

[a]Data acquired in DMSO-d_6.

Table 2. ^{13}C NMR data (δ in ppm) of coumarinyl chalcones **3a–l** (140 MHz, $CDCl_3$, *J* is given in Hz)

No.	3a	3b	3c	3d	3e	3f	3g	3h	3i[a]	3j[a]	3k	3l
OCH_3	—	55.9	55.4	55.5 (4) 55.7 (2)	—	—	—	—	—	—	—	—
2′	159.3	159.2	159.3	159.4	159.4	159.4	159.2	159.3	158.4	158.3	159.1	159.4
3′	125.3	125.7	127.6	126.2	125.0	125.2	125.2	125.1	125.6	125.8	125.8	125.5
4′	148.1	147.6	147.8	147.4	148.4	148.4	148.3	148.2	146.8	146.3	147.5	147.8
4a′	118.5	118.6	118.6	118.7	118.5	118.6	118.5	118.5	118.3	118.3	118.5	118.6
5′	130.0	129.4	129.9	129.9	130.2	130.1	130.1	130.0	130.3	130.2	129.8	130.0
6′	125.0	124.8	124.9	124.8	125.0	125.2	125.0	125.0	124.9	125.4	124.8	124.9
7′	134.2	134.0	134.0	133.8	134.4	134.3	134.3	134.4	134.1	133.9	133.9	134.1
8′	116.7	116.7	116.7	116.6	116.8	116.7	116.7	116.7	116.2	116.1	116.6	116.6
8a′	155.2	155.2	155.1	155.1	155.3	155.3	155.2	155.2	154.4	154.3	155.1	155.2
9′	186.5	186.9	186.3	186.8	186.2	186.3	186.5	186.3	187.3	187.0	187.1	186.3
10′	123.9	124.3	121.6	121.9	126.2	124.4	125.9 (d, 6.7)	123.8 (d, 2.9)	123.8	121.2	124.2	121.5
11′	145.1	140.4	145.0	140.7	140.5	143.5	137.1	143.7	139.8	144.9	140.8	145.3
1	134.8	123.7	125.5	117.2	133.0	133.2	122.9 (d, 12.4)	131.0 (d, 3.2)	121.1	124.9	124.1	127.5
2	128.9	159.0	130.8	160.6	135.8	129.9	161.8 (d, 252.5)	130.8 (d, 10.4)	157.4	130.9	158.4	130.9
3	128.9	111.1	114.4	98.4	130.1	129.2	116.1 (d, 19.4)	116.1 (d, 19.5)	116.1	115.9	112.5	115.1
4	130.8	132.2	161.9	163.5	131.4	136.7	132.2 (d, 8.8)	164.3 (d, 257.3)	132.3	160.4	132.0	161.4
5	128.9	120.7	114.4	105.5	127.1	129.2	124.4 (d, 4.5)	116.1 (d, 19.5)	119.4	115.9	120.6	115.1
6	128.9	129.9	130.8	131.2	128.1	129.9	129.2 (d, 3.0)	130.8 (d, 10.4)	128.9	130.9	129.4	130.9
1″	—	—	—	—	—	—	—	—	—	—	65.6	65.0
2″	—	—	—	—	—	—	—	—	—	—	119.6	119.1
3″	—	—	—	—	—	—	—	—	—	—	137.9	138.8
4″	—	—	—	—	—	—	—	—	—	—	18.4	18.2
5″	—	—	—	—	—	—	—	—	—	—	25.9	25.8

[a]Data acquired in DMSO-d_6.

to identify other residual interactions of the test compounds. An essential feature of the binding site is hydrogen bonding and aromatic π–π stacking interactions. The 2D structures of the molecules were converted to energy minimized 3D structures for in silico protein–ligand docking calculations.

Results and Discussion

Synthesis

Coumarinyl chalcones **3a–l** were synthesized in a two-step reaction, which involved the synthesis of 3-acetylcoumarin, which was synthesized by the Knoevenagel condensation of 2-hydroxybenzaldehyde and ethyl acetoacetate (Scheme 1). A mild base such as piperidine removes the alpha proton of the methylene group between the two carbonyl groups, which make it very acidic. The carbonyl group of the ester then undergoes enolisation, which results in the nucleophilic attack of the carbonyl group of benzaldehyde leading to lactone and coumarin formation. The coumarin intermediate was produced in a yield of 90%. In the second step, 3-acetylcoumarin underwent a Claisen–Schmidt condensation with chloro, fluoro, hydroxy and methoxy benzaldehydes **2a–j** to produce the coumarinyl chalcones **3a–j**. All compounds were yellow precipitates with yields in excess of 80%. The 2-fluoro coumarinyl chalcone **3g** and the 2-*O*-prenylated and 4-*O*-prenylated coumarinyl chalcones, **3k** and **3l** were synthesized for the first time in this work. For the novel prenylated coumarinyl chalcones **3k** and **3l**, 2- and 4-hydroxybenzaldehdyes were each

Table 3. Minimum bactericidal concentrations (MBC) of the test compounds (mM) against two gram +ve and two gram −ve bacterial species and a *Candida* species

Compound	Substitution	*S. aureus*	MRSA	*K. pneumonia*	*E. coli*	*C. albicans*
Ciprofloxacin	-	0.0018	0.0018	0.037	0.0018	0.0074
Ampicillin	-	0.056	0.89	0.89	0.89	1.8
Chalcone	-	9	18	-	-	9
3c	4-OCH_3	33	-	-	-	-
3d	4-Cl	-	-	-	-	32
3e	2-F	34	-	-	-	-
3g	2-OH	32	-	-	-	-
3i	2-OPr	-	27	-	-	-

Hyphen denotes no activity at the highest concentration tested.

Table 4. Docking scores of **3a–l** against trypsin-digested PBP 2X. Binding energies are calculated using Autodock

Compound	(Autodock) Binding energy Kcal mol^{-1}	Intermolecular energy Kcal mol^{-1}	Number of hydrogen bonds	Residues involved in hydrogen bonding	Active residues near the gate of active site of PBP2X
3a	−5.75	−8.73	2	ASN397 GLN552	Ala551, Ser337, Ser558, Thr550, Gly336, Phe550
3b	−6.32	−9.22	2	ASN397 THR550	Asp373, Ser395, Asn397, Gly336, His394, Trp374
3c	−6.20	−9.18	2	ASN397 GLN552	Gln452, Thr550, Glu378, Trp374, Tyr561
3d	−6.65	−9.26	3	Gln552 Arg372 ASN397	Gly336, Gly451 Thr550
3e	−5.75	−8.73	2	ASN397 THR550	Ser395, Gly549, Tyr561, Gly451, Ser548,
3f	−5.60	−8.58	2	ASN397 GLN552	Ser337, Thr550, Ala551, Phe450, Gln452, Ser395,
3g	−5.99	−8.97	2	ASN397 THR550	Ser548,Ser395, Trr561,Phe450, Glu452, Gly549.
3h	−5.80	−8.78	2	ASN397 GLN552	Ser337, Ser548, Phe450, Ala551, Thr550, Gly549
3i	−6.90	−9.88	3	ASN397 THR550 GLN552	Ser395, Ser 548, Ser337, Gly451
3j	−6.44	−9.43	3	SER337 TRP374 GLN552	Lys340, Asp375, Asp373
3k	−7.74	−10.56	2	ASN397 GLN552	Gln452, Thr370, Arg372, Glu334, Thr550, Asp373
3l	−7.73	−10.52	2	SER337 SER395	His394, Ser337, Glu334, Gln552, Thr550, Trp374
AM[a]	−8.04	−10.13	6	Glu378, Asn377, Thr550, Ser337, Ser395, Ser548	Thr526, Asn397, Trp374, Asp373,
CFD[b]	−8.75	−11.44	6	Thr550, Ser395, ser337, Gln452, Glu334, Gln552.	Ser548, Gly549, Tyr561, Ala551, Thr526.

[a]Amoxicillin.
[b]Cefditoren.

treated with prenyl bromide to form the *O*-prenylated intermediates, **2k** and **2l** before being condensed with 3-acetyl coumarin. Potassium carbonate was used as a base to abstract the hydroxyl proton and to neutralize the HBr formed during the reaction.

Structural elucidation

The acetylcoumarin intermediate was identified by its characteristic H-4′ singlet resonance at δ 8.47, a lactone carbonyl resonance at δ 159.3 (C-2′) and aromatic proton resonances at δ 7.29 to 7.64 (H-5′–H-8′). The carbon resonances for the acyl group present occurred at δ 195.5 (C-9′) and δ 30.5 (CH_3). Formation of the chalcone was indicated by a pair of doublets in the region between δ 7.81 and δ 8.29. In the case of compounds **3c**, **3g** and **3l**, the H-10′ and H-11′ resonances had almost similar chemical shifts in $CDCl_3$ because of the electronic effects of the different substituents. To explore this further, we acquired a NMR sample of **3c** in DMSO-d_6 to see if these proton resonances would separate. Interestingly, they did. These resonances now separated at δ 7.51 (H-10′) and δ 7.73 (H-11′), indicating that these protons were able to interact with the solvent. Resonance effects of the α,β-unsaturated carbonyl group indicated that H-10′ is more shielded than H-11′; however, we have observed that in three of the compounds, **3a** (unsubstituted), and the two *para* substituted halogenated compounds, **3f** (4-Cl) and **3h** (4-F), the H-10′ resonance appears downfield to H-11′. In all other compounds, H-10′ is more shielded which are consistent with resonance effects.

The full structural elucidation of all the synthesized molecules **3a–3l** is given in Tables 1 and 2.

Anti-bacterial activity

Compounds **3a–3l** were tested for their antibacterial activity against two gram positive, *S. aureus* species (ATCC 29263 and ATCC BAA-1683), the latter of which was methicillin resistant *S. aureus*, and two gram negative bacteria, *K. pneumonia* ATCC 31488 and *E. coli* ATCC 25922 as well as one fungal species, *C. albicans* ATCC 10231. Along with these compounds, chalcone (1,3-diphenylprop-2-enone) and the precursor, acetylcoumarin were also tested in the same assays for comparison in order to see whether adding a coumarin moiety to the chalcone increased activity or whether the chalcone moiety had a positive influence on the antibacterial action of the compounds. The results are contained in Table 3**.**

In general, the compounds were not as active as the ampicillin and ciprofloxacin standards; however, chalcone showed bactericidal activity of between 9 and 18 mM and five of the coumarinyl chalcones showed bactericidal activity of between 27 and 34 mM in at least one of the *Staphyloccus* species or *C. albicans*. The compounds were totally inactive to the Gram-negative species. Chalcone itself was the most active and showed the broadest spectrum of activity, being active against both *Staphyloccus* species and *C. albicans*. The activity of chalcone against MRSA was 20-fold lower than that of ampicillin. In the fungal species, chalcone showed a fivefold lower activity than ampicillin.

The coumarin moiety did not enhance the activity of chalcone. In fact, acetylcoumarin itself was totally inactive to all the microbial species tested against. Adding particular substituted chalcone moieties to this increased the activity somewhat. In particular, the 4-OCH_3, 2-F and 2-OH (**3c**, **3e** and **3g**) derivatives were now active against *S. aureus* ATCC 29263 between 32 and 34 mM and **3i** (the *O*-prenylated derivative) was active against MRSA at 27 mM. The 4-Cl derivative (**3d**) was the only coumarinyl chalcone to show any activity against *Candida*. These results also indicated that the type and position of the substituent were important for antibacterial activity.

Molecular docking studies

Molecular docking analysis for the synthesized coumarinyl chalcones **3a–3l** was carried out with the crystal structure of cefditoren (CDS) bound to the active site of PBP 2X to identify the variations in binding affinity using Autodock4 software. The crystal

structure of this complex was identified in the Protein data bank as PDB ID: **2Z2M**. The PDB structure **2Z2M** bound to the inhibitor CDS shows a true binding site for each of the subunits and was considered as the centre of search space for docking. The molecular docking results are summarized in Table 4. For the test compounds **3a** to **3l**, the Autodock score ranged from −5.60 to −7.74 Kcal mol^{-1}, while the Autodock score of the standard drugs Amoxicillin and CDS was −8.04 and −8.75 Kcal mol^{-1} respectively. Based on the Autodock score, compounds **3i** (2-hydroxycoumarinyl chalcone), **3k** (2-oxyprenylcoumarinylchalcone) and **3l** (4-oxyprenylcoumarinylchalcone) with Autodock scores of −6.90, −7.74 and −7.73 Kcal mol^{-1} respectively showed the best binding affinity using the criteria that the lower the binding energy score the higher the binding affinity.

The mode of interaction between all docked synthesized compounds and the trypsin-digested PBP 2X receptor were created with Ligplot software. Compound **3k** with the best binding affinity docked in its best conformation into the binding site of trypsin-digested PBP 2X is shown in Fig. 1. This model was considered as a clue to obtaining a clear picture of the relative arrangement of binding interaction sites. The hydrogen bond interactions with the residues (in green) are shown by dashed lines, and hydrophobic contacts are represented by an arc with spokes radiating toward the ligand atoms they come into contact with. As can be seen from Fig. 2 compound **3i** fits nicely into the enzyme, with the α,β-unsaturated carbonyl hydrogen bonding to Asn 397, the oxygen of the coumarin hydrogen bonding to Thr 550 and the 2-OH group to Gln 552. Compound **3k** fits nicely into the pocket in the enzyme with hydrogen bonding from the α,β-unsaturated carbonyl to Asn 397 and from the heteratomic oxygen of the coumarin to Gln 552. Hydrogen bonding between the α,β-unsaturated carbonyl group with the Asn 397 residue could be a reason why the chalcone scaffolds are more active than the just the coumarin alone.

Conclusion

Claisen–Schmidt condensation was used to synthesize 12 coumarinyl chalcones from coumarinyl acetophenone and benzaldehyde precursors. The substituents on the benzaldehdye derived aromatic ring were hydroxy, methoxy, chloro, fluoro and prenyloxy groups, which were substituted at the 2 and 4 positions. The ^{1}H and ^{13}C NMR resonances of all synthesized compounds were unambiguously assigned and will provide a basis for the structural determination of similar compounds. Two of the compounds in the series, **3k** (2-oxyprenylcoumarinyl chalcone) and **3l** (4-oxyprenylcouma rinyl chalcone) were novel derivatives that showed a binding affinity close to the standard amoxicillin and CDS. The coumarinyl moiety of the chalcone did not enhance the antimicrobial activity of chalcone, but instead led to worse activity.

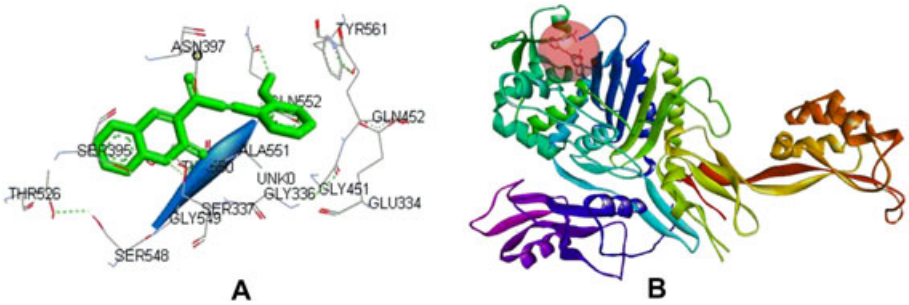

Figure 1. Compound **3k** docked in its best conformation into the binding site of trypsin-digested PBP 2X; Hydrogen bonds are represented by broken lines (blue). (A) Binding mode of compound **3k** showing interactions with the protein, (B) **3k** fitting into the binding pocket of the protein.

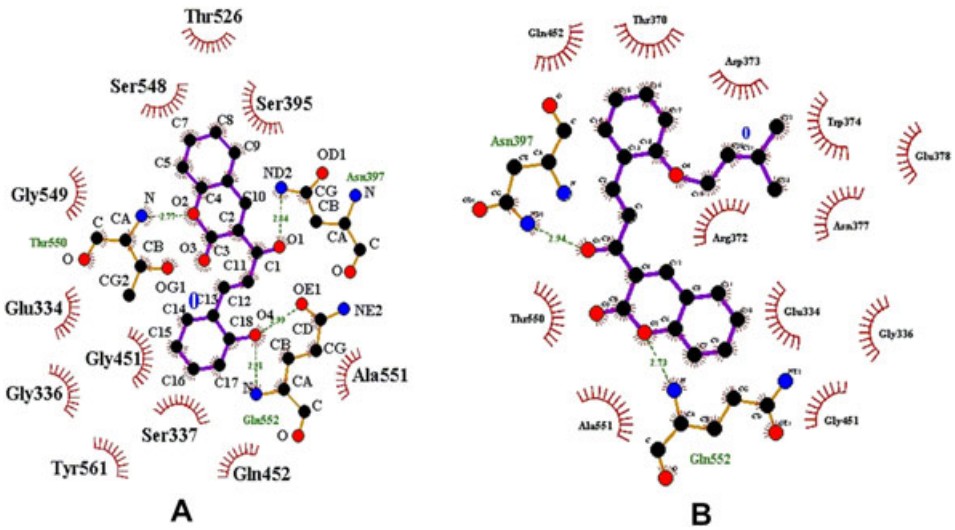

Figure 2. Schematic diagrams of protein-ligand interactions. (A) Structure of docked ligand 3i-2Z2M complex (B) Structure of docked ligand 3k-2Z2M complex.

Acknowledgement

Thrineshan Moodley thanks the National Research Foundation in South Africa for a doctoral scholarship.

References

[1] G. J. B. Gnonlonfin, A. Sanni, L. Brimer. *Crit. Rev. Plant Sci.* **2012**, *31*, 47–56.
[2] R. M. P. Gutierrez, A. Muñiz-Ramirez, J. V. Sauceda. *Afr. J. Pharm. Pharmacol.* **2015**, *9*, 237–257.
[3] K. N. Venugopala, V. Rashmi, B. Odhav. *BioMed Res. Int.* **2013**, *2013*, Article ID 963248 14.
[4] V. R. Yadav, S. Prasad, B. Sung, B. B. Aggarwal. *Int. Immunopharmacol.* **2011**, *11*, 295–309.
[5] P. K. Jain, H. Joshi. *J. Appl. Pharm. Sci.* **2012**, *2*, 236–240.
[6] D. P. Kamat, S. G. Tilve, V. P. Kamat, J. K. Kirtany. *Org. Prep. Proced. Int.* **2015**, *47*, 1–79.
[7] D. K. Mahapatra, V. Asati, S. K. Bharti. *Eur. J. Med. Chem.* **2015**, *92*, 839–865.
[8] A. Shakeri, M. Iranshahy, M. Iranshahi. *J. Asian Nat. Prod. Res.* **2014**, *16*, 884–889.
[9] P. Singh, A. Anand, V. Kumar. *Eur. J. Med. Chem.* **2014**, *85*, 758–777.
[10] A. I. Essawy, M. Elkady, A. Y. Mohamed. *Indian J. Chem., Sect. B: Org. Chem. Incl. Med. Chem.* **1980**, *19B*, 567–570.
[11] B. L. Narayanan, L. A. P. Rajkumar, A. Arunlanandham, N. S. Babu, T. Gayathri, A. Raju. *Int. J. Pharm. Res.* **2012**, *3*, 474–478.
[12] S. Vazquez-Rodriguez, S. Serra, Y. Santos, L. Santana. *Proceedings of the 14th Int. Electron. Conf. Synth. Org. Chem.* **2010**, *14*, b001. http://sciforum.net/conference/ecsoc-14/paper/403
[13] G. Xi, Z. Liu. *Eur. J. Med. Chem.* **2013**, *68*, 385–393.
[14] G. J. Kharadi, K. D. Patel. *J. Therm. Anal. Calorim.* **2009**, *96*, 1019–1028.
[15] S. Khode, V. Maddi, P. Aragade, M. Palkar, K. P. Ronad, S. Mamledesai, A. H. M. Thippeswamy, D. Satyanarayana. *Eur. J. Med. Chem.* **2009**, *44*, 1682–1688.
[16] O. O. Ajani, O. C. Nwinyi. *J. Heterocycl. Chem.* **2010**, *47*, 179–187.
[17] S. S. Gholap, U. P. Deshmukh, M. S. Tambe. *Iranian J. Catal.* **2013**, *3*, 171–176.
[18] C. Seidel, M. Schnekenburger, C. Zwergel, F. Gaascht, A. Mai, M. Dicato, G. Kirsch, S. Sergio Valente, M. Diederich. *Bioorg. Med. Chem. Lett.* **2014**, *24*, 3797–3801.
[19] N. Hamdi, C. Fischmeister, M. C. Puerta, P. Valerga. *Med. Chem. Res.* **2003**, *20*, 522–530.
[20] B. S. Jayashree, S. Yusuf, D. V. Kumar. *Asian J. Chem.* **2009**, *21*, 5918–5922.
[21] H. V. Burghate, P. B. Raghuwanshi. *J. Applicable Chem.* **2014**, *3*, 2378–2383.
[22] J. Patel, H. Dholariya, K. Patel, J. Bhatt, K. Patel. *Med. Chem. Res.* **2014**, *23*, 3714–3724.
[23] V. R. Avupati, R. P. Yejella. *World J. Pharm. Pharm. Sci.* **2014**, *3*, 1713–1742.
[24] A. Behrami. *Orient. J. Chem.* **2014**, *30*, 1747–1752.
[25] J. Grover, S. M. Jachak. *RSC Adv.* **2015**, *5*, 38892–38905.
[26] L. Han, B. Huang, Z. Xiong, C. Yan. *J. Med. Plants Res.* **2015**, *9*, 435–444.
[27] J. Wu, C. Cheng, L. Shen, Z. Wang, S. Wu, W. Li, S. Chen, R. Zhou, P. Qiu. *Int. J. Mol. Sci.* **2014**, *15*, 18525–18539.
[28] P. Zhong, L. Wu, Y. Qian, Q. Fanga, D. Liang, J. Wang, C. Zeng, Y. Wang, G. Liang. *Biochim. Biophys. Acta* **2015**, *1852*, 1230–1241.
[29] A. V. Babu, R. Navudu, G. Trimurtulu, B. H. Babu. *Med. Chem. Res.* **2014**, *23*, 877–881.
[30] D. Kumar, K. K. Raj, S. V. Malhotrab, D. S. Rawat. *Med. Chem. Commun.* **2014**, *5*, 528–535.
[31] R. El-Haggar, R. I. Al-Wabli. *Molecules* **2015**, *20*, 5374–5391.
[32] S. Wang, Y. Yin, X. Wu, F. Qiao, S. Sha, P. Lv, J. Zhao, H. Zhu. *Bioorg. Med. Chem.* **2014**, *22*, 5727–5737.
[33] K. Divekar, S. Swamy, V. Murugan. *Int. J. Pharm. Phytopharm. Res.* **2014**, *3*, 447–450.
[34] J. M. Andrews. *J. Antimicrob. Chemother.* **2001**, *48*, 5–16.
[35] M. J. Frisch, G. W. Trucks, H. B. Schlegel, G. E. Scuseria, M. A. Robb, J. R. Cheeseman, G. Scalmani, V. Barone, B. Mennucci, G. A. Petersson, H. Nakatsuji, M. Caricato, X. L.,. H. P. Hratchian, A. F. Izmaylov, J. Bloino, G. Zheng, J. L. Sonnenberg, M. Hada, M. Ehara, K. Toyota, R. Fukuda, J. Hasegawa, M. Ishida, T. Nakajima, Y. Honda, O. Kitao, H. Nakai, T. Vreven, J. A. Montgomery Jr., J. E. Peralta, F. Ogliaro, M. Bearpark, J. J. Heyd, E. Brothers, K. N. Kudin, V. N. Staroverov, R. Kobayashi, J. Normand, K. Raghavachari, A. Rendell, J. C. Burant, S. S. Iyengar, J. Tomasi, M. Cossi, N. Rega, J. M. Millam, M. Klene, J. E. Knox, J. B. Cross, V. Bakken, C. Adamo, J. Jaramillo, R. Gomperts, R. E. Stratmann, O. Yazyev, A. J. Austin, R. Cammi, C. Pomelli, J. W. Ochterski, R. L. Martin, K. Morokuma, V. G. Zakrzewski, G. A. Voth, P. Salvador, J. J. Dannenberg, S. Dapprich, A. D. Daniels, Ö. Farkas, J. B. Foresman, J. V. Ortiz, J. Cioslowski, D. J. Fox, *Gaussian 09, Revision E.01*, Gaussian, Inc., Wallingford CT, **2009**.

Supporting Information

Additional supporting information may be found in the online version of this article at the publisher's web site.

